

# Calculations of the thermal conductivities of ionic materials by simulation with polarizable interaction potentials

Norikazu Ohtori,<sup>1</sup> Mathieu Salanne,<sup>2</sup> and Paul A. Madden<sup>3,a)</sup>

<sup>1</sup>Graduate School of Science and Technology, Niigata University, Niigata 950-2181, Japan

<sup>2</sup>UPMC Univ Paris 06, UMR 7612, LI2C, F-75005 Paris, France  
and CNRS, UMR 7612, LI2C, F-75005 Paris, France

<sup>3</sup>Department of Materials, University of Oxford, Parks Road, Oxford OX1 3PH, United Kingdom

(Received 16 September 2008; accepted 3 February 2009; published online 12 March 2009; publisher error corrected 17 March 2009)

Expressions for the energy current of a system of charged, polarizable ions in periodic boundary conditions are developed in order to allow the thermal conductivity in such a system to be calculated by computer simulation using the Green–Kubo method. Dipole polarizable potentials for LiCl, NaCl, and KCl are obtained on a first-principles basis by “force matching” to the results of *ab initio* calculations on suitable condensed-phase ionic configurations. Simulation results for the thermal conductivity, and also other transport coefficients, for the melts are compared with experimental data and with results obtained with other interaction potentials. The agreement with experiment is almost quantitative, especially for NaCl and KCl, indicating that these methodologies, perhaps with more sophisticated forms for the potential, can be used to predict thermal conductivities for melts for which experimental determination is very difficult. It is demonstrated that the polarization effects have an important effect on the energy current and are crucial to a predictive scheme for the thermal conductivity. © 2009 American Institute of Physics. [DOI: 10.1063/1.3086856]

## I. INTRODUCTION

There is a resurgence of interest in calculating the thermal conductivity of ionic systems using realistic models of the ionic interactions; the interest derives from several sources. Lack of knowledge of the thermal conductivity of minerals at the temperatures and pressures relevant to the earth’s mantle is a significant barrier to quantitative understanding of the heat flux from the earth’s core to the surface.<sup>1</sup> Similar information on the performance of ceramics at high temperatures is required for the design of improved thermal barrier coatings, for use in jet engines, etc.<sup>2</sup> Several new energy-related technologies require information on the thermal conductivity of ionic melts at high temperatures. In the Generation IV nuclear reactor concepts, the advanced high-temperature reactor<sup>3</sup> and the molten salt reactor,<sup>4</sup> a molten fluoride acts as coolant. Molten salts are also proposed for heat exchangers in solar thermal and fusion power plants. In these technologies, values for the thermal conductivity are required for engineering calculations of the proposed plant performance.

The measurement of the thermal conductivity under the extreme physical and chemical conditions pertinent to these applications is very challenging; the difficulties in measuring the thermal conductivities of ionic melts are discussed by Nagasaka *et al.*<sup>5</sup> For example, to the best of our knowledge, no measurements have been made for fluoride melts of interest in some of the above-mentioned applications. There is, however, good reason to hope that reliable values for the materials of interest can be predicted from computer simula-

tions. For melts this requires the evaluation of the time correlation functions of the heat flux<sup>6</sup> using an appropriate, realistic description for the interionic interactions. Alternatively, the thermal conductivity can be obtained from the calculation of the temperature profile in a simulation cell subjected to a temperature gradient.<sup>7,8</sup> This non-equilibrium molecular dynamics (NEMD) method does not require an expression for the heat flux, although Galamba *et al.* have discussed problems in applying it for calculations in multi-component systems.<sup>9</sup> In solids, it is conventional to think of obtaining the thermal conductivity from the anharmonic interactions between phonons. At the very high temperatures of interest in thermal barrier coatings and the earth’s mantle, a quantum description of the ion dynamics is irrelevant and the anharmonic effects are so strong that the phonon mean-free paths become short compared to the lengths of typical simulation cells: under these circumstances, calculation of the thermal conductivity with the same classical simulation methods used for a melt is appropriate.

The method of choice for predicting the thermal properties of a melt would normally be *ab initio* molecular dynamics (MD) since the amount of empirical information needed to set up the calculation is minimal. However, as we will see, obtaining the requisite statistical precision on samples of adequate size puts the calculations beyond what can be currently achieved with these methods. Recently, we have developed techniques<sup>10,11</sup> to parametrize interaction potentials for halides and oxides directly from *ab initio* electronic structure calculations. In order to provide an accurate, transferable description of the interactions, the potentials are polarizable and, in the oxide case, allow the ions to be deformed by interactions with their neighbors. With these

<sup>a)</sup>Electronic mail: paul.madden@queens.ox.ac.uk.

models we have predicted values for transport properties of melts and solids on a nonempirical basis with excellent agreement with experiment; the transport properties include the viscosity and electrical conductivity which are expected to present similar challenges to the thermal conductivity. In this paper we will show how the thermal conductivity can be evaluated for potentials of this type and predict values for alkali chloride melts, for which experimental values have been obtained from forced-Rayleigh scattering experiments.<sup>5</sup>

In ionic systems the long-ranged Coulombic interactions are expected to make important contributions to the heat flux. In computer simulations with periodic boundary conditions, the Coulombic interactions are handled by the Ewald summation.<sup>12,13</sup> An expression for the heat flux in a system of charged particles in periodic boundaries was first provided by Bernu and Viellefosse in 1978;<sup>14</sup> however, this expression has been criticized in more recent work<sup>9,15</sup> and an alternative expression suggested (although without formal derivation). We begin this paper by discussing the appropriate form for the heat flux of charged particles in periodic boundary conditions. A new derivation is provided and we resolve the controversy about the appropriate form. We then generalize this derivation to allow for induced multipoles in order to work with the polarizable potentials which, as we will show, are essential for the accurate representation of the *ab initio* forces.

We then briefly describe the construction of the *ab initio* polarizable potentials for the alkali chlorides; in future work we will use the same methodology to generate potentials for other materials. In the remaining sections, we will give results for the thermal conductivity as well as calculated values for other transport coefficients, where comparison with experiment supports the quality of the potentials. We will also illustrate the significance of the polarization effects for the calculation of the thermal conductivity and compare our results with the *ab initio* potentials with those obtained with the Fumi–Tosi effective pair potentials<sup>16,17</sup> using the same methodology. It should be noted at the outset that the latter potentials have been shown by many workers to reproduce many of the structural, thermodynamic, and transport properties of the alkali halides extremely well (although the discrepancies between the calculated and measured thermal conductivity values show a larger systematic deviation than has been found for these other properties). We already know that the polarization effects induce only small changes in the structure<sup>18</sup> and thermodynamics<sup>19</sup> of these MX stoichiometry materials. From this perspective, it might seem sensible to illustrate the calculations on MX<sub>2</sub> and MX<sub>3</sub> systems where the polarization effects are substantial: the reason for focusing on the alkali halides is that they are so well studied both experimentally and in simulation and are appropriate for testing a method which can be applied to these other, more complex cases.

## II. THE CALCULATION OF THE THERMAL CONDUCTIVITY

In a binary ionic system the thermal conductivity may be calculated from the integrals of time correlation functions of the energy and charge currents,<sup>14,15</sup>

$$\lambda = T^{-2} \left( L_{ee} - \frac{L_{ez}^2}{L_{zz}} \right), \quad (1)$$

where  $T$  is the temperature and

$$L_{ab} = \frac{1}{k_B} \int_0^\infty dt C_{ab}(t). \quad (2)$$

$$C_{ab}(t) = \frac{1}{3V} \langle \vec{j}_a(t) \cdot \vec{j}_b(0) \rangle.$$

Here  $\vec{j}_e$  and  $\vec{j}_z$  are the low-wavevector limits of the spatial Fourier transforms of the energy and charge currents,  $V$  is the volume, and  $k_B$  is Boltzmann's constant.  $\vec{j}_z$  is given by

$$\vec{j}_z(t) = \sum_i z_i \vec{v}_i(t), \quad (3)$$

where  $z_i$  and  $\vec{v}_i$  are the charge and velocity of particle  $i$ . An expression for the energy current  $\vec{j}_e(\vec{r}, t)$  is obtained from the time derivative of the energy density,

$$\dot{e}(\vec{r}, t) = -\vec{\nabla} \cdot \vec{j}_e(\vec{r}, t), \quad (4)$$

and taking the spatial Fourier transform gives the desired expression for  $\vec{j}_e$ . For a system in which the interactions between the particles are described by *short-range* pair potentials  $u_{ij}^{\text{sr}}(r_{ij})$ ,  $\vec{j}_e$  is given by<sup>6,14</sup>

$$\vec{j}_e = \sum_i \left( \frac{1}{2} m_i v_i^2 + \frac{1}{2} \sum_{j \neq i} u_{ij}^{\text{sr}} \right) \vec{v}_i + \frac{1}{2} \sum_{i, j \neq i} \vec{v}_i \cdot \vec{r}_{ij} \vec{f}_{ij}^{\text{sr}}, \quad (5)$$

where  $m_i$  is the mass and  $\vec{v}_i$  the velocity of particle  $i$  and  $\vec{f}_{ij}^{\text{sr}}(\vec{r}_{ij}) = -\vec{\nabla}_{ij} u_{ij}^{\text{sr}}(r_{ij})$  is the force on particle  $i$  due to  $j$  arising from the short-range potential. The first of these sums reflects a convective contribution to the energy flow, whereas the second may be called a “virial-like” term, by analogy with the virial contributions to the stress tensor which involve a similar function of the position variables.

Two problems arise in generalizing Eq. (5) to deal with the charged, polarizable ions of interest. Firstly, the form of the terms involving the interaction potential for charge-charge interactions in periodic boundary conditions has proven controversial because the short-range assumption invoked in the derivation of Eq. (5) is inapplicable.<sup>14</sup> Secondly, polarization effects give a many-body character to the interaction potential; to the best of our knowledge no expressions for the energy flux for polarizable particles have been obtained previously.

### A. Charge-charge contributions to the energy current

Bernu and Viellefosse<sup>14</sup> addressed the first of these problems and derived an expression for the energy flux, as well as expressions for the energy density and the stress tensor, in a system of charged particles in a neutralizing background (a one-component plasma) by using the Ewald summation method. This expression has been used to represent the charge-charge contributions to the energy current in several calculations of the thermal conductivity of molten salts.<sup>20</sup> Recently, these expressions have been criticized as

being inconsistent with those normally used in computer simulation, obtained after the reformulation of de Leeuw *et al.*<sup>21</sup> of the Ewald summation, and an alternative expression for the energy current has been proposed.<sup>15,22</sup>

In the Ewald method, the charge-charge contribution to the force on an ion may be written

$$\vec{f}_i = \sum_{j \neq i} \vec{f}_i^{\text{real}}(\vec{r}_{ij}, \alpha) + \sum_j \vec{f}_i^{\text{recip}}(\vec{r}_i, \vec{r}_j, \alpha), \quad (6)$$

where the first term, the “real-space” term, involves a modified coulombic force. Similarly, the expression for  $\vec{j}_e$  may be written as a sum of a real space and a reciprocal space contribution

$$\vec{j}_e = \vec{j}_e^{\text{real}} + \vec{j}_e^{\text{recip}}. \quad (7)$$

Because, in practice, the range of the real-space part of the Coulomb force is restricted to be less than the size of the simulation cell by an appropriate choice of the Ewald parameter  $\alpha$ , the real-space contributions to the energy flux can be written in a virial-like form, as in Eq. (5). This gives

$$\begin{aligned} \vec{j}_e^{\text{real}} = & \sum_i \vec{v}_i \left( \frac{1}{2} m_i v_i^2 + \epsilon_i^c + \frac{1}{2} \sum_{j \neq i} u_{ij}^{\text{sr}} \right) \\ & + \frac{1}{2} \sum_{i, j \neq i} \vec{v}_i \cdot \vec{r}_{ij} (\vec{f}_{ij}^{\text{sr}} + \vec{f}_{ij}^{\text{real}}), \end{aligned} \quad (8)$$

where  $\epsilon_i^c$  is the Coulombic contribution to the energy of  $i$ ,<sup>12</sup>

$$\begin{aligned} \epsilon_i^c = & -\frac{\alpha}{\sqrt{\pi}} z_i^2 + \frac{1}{2} \sum_j \sum_{\vec{k} \neq 0} z_i z_j \frac{4\pi \exp(-k^2/4\alpha^2 - i\vec{k} \cdot \vec{r}_{ij})}{V k^2} \\ & + \frac{1}{2} \sum_{j \neq i} z_i z_j \frac{\text{erfc}(\alpha r_{ij})}{r_{ij}}, \end{aligned} \quad (9)$$

and the real-space Coulomb force between  $i$  and  $j$ ,  $\vec{f}_{ij}^{\text{real}}$ , is given by

$$\vec{f}_{ij}^{\text{real}} = z_i z_j \frac{\vec{r}_{ij}}{r_{ij}^2} \left( \frac{\text{erfc}(\alpha r_{ij})}{r_{ij}} + \frac{2\alpha}{\sqrt{\pi}} \exp(-\alpha^2 r_{ij}^2) \right). \quad (10)$$

For the contribution to the energy flux from the remaining “reciprocal space” contribution to the charge-charge force, it has been suggested that, because of the similarity between the expressions for the configurational contributions to the energy flux and stress tensor for short-range interactions, the reciprocal space term should contain the same function of ionic positions as reciprocal space contributions to the stress tensor. Note that the stress tensor may be obtained, unambiguously by considering the change in energy on straining the simulation cell.<sup>23</sup> By these means the following expression for  $\vec{j}_e^{\text{recip}}$  is obtained:

$$\begin{aligned} \vec{j}_e^{\text{recip}} = & \frac{1}{2} \sum_{\vec{k} \neq 0} \sum_{ij} \exp(-i\vec{k} \cdot \vec{r}_{ij}) z_i z_j \frac{4\pi \exp(-k^2/4\alpha^2)}{V k^2} \\ & \times \left[ \vec{v}_i - (\vec{k} \cdot \vec{v}_i) \vec{k} \left( \frac{k^2 + 4\alpha^2}{2\alpha^2 k^2} \right) \right]. \end{aligned} \quad (11)$$

This expression has been used by Galamba *et al.*<sup>9,15</sup> to calculate the thermal conductivity of molten alkali chlorides

using the Fumi–Tosi potentials and obtain agreement with NEMD values and quite good agreement with experiment.

The argument that leads to Eq. (11) seems to us *a priori* unsatisfactory; the reciprocal space contributions to the force involve not only the direct interaction of  $i$  with the nearest image of  $j$  but also its interaction with all the periodic images of  $i$  and  $j$ . The presence of the ionic velocity in the expression for the energy current for short-range interactions, Eq. (5), means that this term is fundamentally different to the purely configurational virial contribution to the stress tensor when non-nearest image interactions are involved.

We have, therefore, derived an expression for the energy current for a system of (nonpolarizable) ions starting from the Ewald expression for the Coulomb energy normally used in computer simulations. The derivation is given in Appendix A. We have separated the Coulomb energy convective term and the real-space Coulomb force contribution as in Eq. (8). The result we obtain for the reciprocal space energy flux is exactly that given in Eq. (11).

As Galamba *et al.* noted,<sup>15</sup> the net expression for the energy current is of a very different form to that given by Bernu and Vieillefosse.<sup>14</sup> Since the latter expression has been used in other calculations of the thermal conductivity of molten salts we have analyzed the relationship to Eqs. (8) and (11) in Appendix B. We find that, in practical applications, the two formulations will lead to the same results. Bernu and Vieillefosse appear to have an error in certain Ewald self-energy terms compared to more recent<sup>21</sup> derivations of the Ewald energy. However, these terms only contribute to the energy current in a binary system to the extent that each species can have a nonzero net velocity, and such terms are largely “projected out” by the  $L_{zz}^2/L_{zz}$  factor in Eq. (1). The other differences between the two expressions are purely superficial and arise because the real and reciprocal space contributions to  $\epsilon_i^c$  and the energy flux are partitioned in different ways.

## B. Energy current for a system of polarizable ions

To describe a system of polarizable ions we introduce the instantaneous values of the dipole on each ion  $\vec{\mu}_i$  as an additional dynamical variable and use an expression for the total energy which is<sup>10,24</sup>

$$\begin{aligned} H = & \left[ \sum_i \frac{1}{2} m_i v_i^2 + \frac{1}{2} \sum_{j \neq i} \left( u_{ij}^{\text{sr}} + \frac{z_i z_j}{r_{ij}} \right) \right] + \frac{1}{2} \sum_{i, j \neq i} \\ & \times (\vec{\mu}_i \cdot \tilde{\mathbf{T}}_{ij}^{(1)} z_j - \vec{\mu}_j \cdot \tilde{\mathbf{T}}_{ij}^{(1)} z_i - \vec{\mu}_i \cdot \mathbf{T}_{ij}^{(2)} \cdot \vec{\mu}_j) + \sum_i \frac{1}{2} k_i \mu_i^2. \end{aligned} \quad (12)$$

Here the term in square brackets includes the kinetic energy and the short-range and charge-charge interactions, whose contributions to the energy flux have been discussed above. The final term is a Drude-type representation of the energy involved in polarizing an ion, with  $k_i$  equal to the reciprocal of the ion’s dipole polarizability. The remaining terms are the charge-dipole and dipole-dipole interactions, with  $\mathbf{T}_{ij}^{(n)}$  an interaction tensor<sup>25</sup> (e.g.,  $\mathbf{T}_{ij}^{(2)} = \vec{\nabla}_{ij} \cdot \vec{\nabla}_{ij} r_{ij}^{-1}$ ). To complete the specification of the system, the values of the dipoles are ob-

tained at each ionic configuration by minimizing  $H$  with respect to the dipole variations. Since the calculation is variational, the forces on the ions may be derived by application of a Hellmann–Feynman theorem from the derivatives of  $H$  with respect to ionic positions and neglecting the derivatives of the dipoles.

In practice, the form of the charge-dipole interaction tensor is modified<sup>10</sup> to allow for short-range contributions to dipole induction, and this is denoted by  $\tilde{\mathbf{T}}^{(1)}$  in Eq. (12), given by

$$\tilde{\mathbf{T}}^{(1)}(\vec{r}_{ij}) = \mathbf{T}^{(1)}(\vec{r}_{ij}) - h_{ij}(r_{ij})\mathbf{T}^{(1)}(\vec{r}_{ij}). \quad (13)$$

Here  $h_{ij}(r)$  is a short-ranged step function<sup>26</sup>

$$h_{ij}(r_{ij}) = c_{ij}e^{-(b_{ij}r_{ij})} \sum_{k=0}^4 \frac{(b_{ij}r_{ij})^k}{k!}, \quad (14)$$

which goes to zero for  $r_{ij} > b_{ij}^{-1}$ . The charge-dipole term therefore contains a long-range part, the first term in Eq. (13), which is handled via the Ewald method in the expressions for the energy current, and a short-ranged term which is treated along with the other short-ranged contributions in real space.

In Appendix C we obtain an expression for the energy flux in this representation for a periodic system of charged, polarizable particles. We form an appropriate energy density, using a standard Ewald representation of the long-ranged contributions to the interactions in such a system, and differentiate with respect to time, as in Eq. (4). The time derivative is interpreted as

$$\frac{d}{dt} = \sum_i \left( v_{i,\alpha} \frac{\partial}{\partial r_{i,\alpha}} + \dot{v}_{i,\alpha} \frac{\partial}{\partial v_{i,\alpha}} \right), \quad (15)$$

that is, there is no term involving the velocities of the dipoles. That this is the correct interpretation can be seen in two ways. Because the dipoles are treated adiabatically, there is no dipole kinetic energy term to appear in  $H$ . If dipole velocities were to be included in the time derivatives of the interaction terms, the energy density would not be conserved, as in Eq. (4) (see Appendices A and C). Alternatively, we can consider an analogous operation of deriving the stress tensor from the time derivative of the momentum density<sup>6</sup> and comparing with the expression obtained by statically deforming the simulation cell and invoking the Hellmann–Feynman result,<sup>27</sup> which involves no assumptions about velocities. The expressions are found to be identical if the time derivative is treated as in Eq. (15).

The explicit derivation of the expression for the energy flux for polarizable ions in periodic boundary conditions is given in Appendix C.  $\vec{j}_e$  for polarizable particles may still be written [Eq. (C11)] as the sum of a real space and reciprocal space contribution, as in Eq. (7). The real-space contribution still contains a convective and virial-like term, although now  $\epsilon_i^c$  [Eq. (C12)] and  $f_{ij}^{\text{real}}$  contain contributions from charge-dipole and dipole-dipole interactions and the Drude-type self-energy. The final form for  $\vec{j}_e^{\text{recip}}$  is given in Eq. (C14).

### III. *AB INITIO* POTENTIALS FOR THE ALKALI CHLORIDES

Polarizable potentials have already been used for the simulation of molten chlorides. These were developed from a combination of *ab initio* calculations and experimental results and could be said to provide a semiempirical representation of the interactions.<sup>28</sup> Those potentials have proven useful for the determination of transport properties such as the diffusion coefficients or the electrical conductivity<sup>18</sup> as well as thermodynamic properties such as the activity coefficients.<sup>29,30</sup>

For this study a new set of parameters was determined on a purely first-principles basis in order to illustrate a procedure that can be applied to systems for which it would be difficult to perform the experimental studies necessary to help parametrize the semiempirical potentials. The potentials consist of a pair potential of Born–Mayer form together with the account of ionic Coulomb and polarization interactions<sup>10,24</sup> summarized above. The pair potential is written

$$V(r_{ij}) = B^{ij}e^{-\alpha^{ij}r_{ij}} - f_{ij}^{(6)}(r_{ij})\frac{C_{ij}^6}{r_{ij}^6} - f_{ij}^{(8)}(r_{ij})\frac{C_{ij}^8}{r_{ij}^8}, \quad (16)$$

where  $C_{ij}^6$  and  $C_{ij}^8$  are the dispersion coefficients and  $f_{ij}^{(n)}$  are dispersion damping functions<sup>26</sup> given by

$$f_{ij}^{(n)}(r_{ij}) = 1 - e^{-(b_{ij}^n r_{ij})} \sum_{k=0}^n \frac{(b_{ij}^n r_{ij})^k}{k!}. \quad (17)$$

We have described elsewhere at some length the parametrization of the polarizable interaction potentials by a generalization of the “force-matching” technique.<sup>10,31</sup> Briefly, we generate several ionic configurations for the system of interest by running MD on a relatively small system (of roughly 100 ions) in periodic boundary with some trial potential. We then perform an *ab initio* electronic structure calculation using a planewave DFT code<sup>32</sup> on each of these configurations and obtain values for the force and dipole on each ion. We then refine the interaction potential by varying its parameters to minimize the difference between the predicted and *ab initio*-calculated values on these configurations. We first fit the polarization parts of the potential to the dipoles and then fit the remaining parts of the potential to the forces. If necessary, a second iteration of the force-matching process can be made by running MD with the fitted potential and repeating the *ab initio* and minimization steps. The quality of the representation of the ionic interactions provided by this process can be systematically improved. We may allow for a more sophisticated representation of the interactions, e.g., by including induced quadrupoles. We may also determine additional, independent constraints on the fitting parameters from the *ab initio* process; for example, we have shown how to fix the ionic polarizabilities independently of the force-matching process.<sup>33,34</sup> These refinements will be examined in future work.

In the present case, we used seven configurations of 120 ions for LiCl, three configurations of 124 ions for NaCl, and three configurations of 100 ions for KCl. These were taken from MD runs at 1300 and 1200 K using the previous semi-

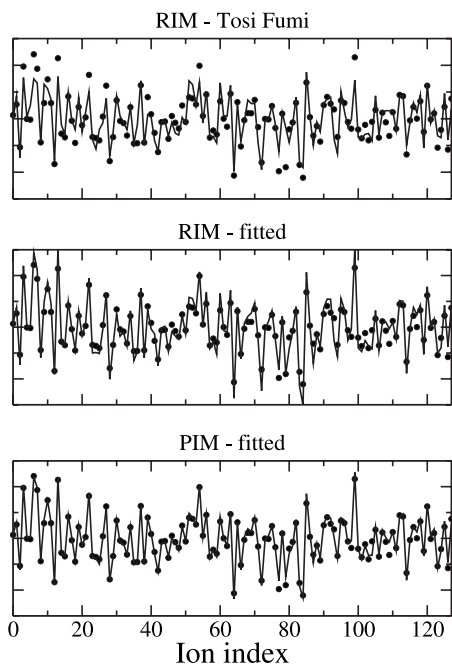


FIG. 1. Results of force matching. The values of the  $x$ -component of the force on each of 128 ions obtained by *ab initio* electronic structure calculations on liquid-phase configurations of NaCl are shown by points and compared with the values predicted by different potentials. The top two panels show the predictions with simple pair potentials [rigid-ion models (RIMs)], the topmost shows the empirically parametrized Fumi–Tosi potential, and the central panel the forces obtained by the best RIM which can be fitted to the *ab initio* data. The bottom panel shows the results obtained with the best dipole polarizable potential, which gives an excellent representation of the *ab initio* forces.

empirical potentials.<sup>18,30</sup> We found that the dipole polarizable potentials, using a fixed in-crystal chloride ion polarizability<sup>35</sup> of 20 a.u.,<sup>8</sup> gave a good representation of the *ab initio* data (see Refs. 10 and 31 for similar examples). The fits on the different systems are performed simultaneously, with the same potentials to represent the Cl–Cl interactions in all three systems, as the objective is to obtain potentials which are transferable and can be used in mixtures as well as the pure materials.

The quality of the representation is illustrated in Fig. 1 where we compare the forces from the fitted potential with the *ab initio* data for one of the configurations for NaCl. The figure shows the comparison of the  $x$ -component of the *ab*

*initio* forces for the ions of one configuration with the values predicted by the fitted potential. The agreement is seen to be uniformly good and is characterized by a value of the objective function for the fit of  $\chi^2=0.118$  for the forces. The quality of the agreement found for the other alkalis was similar ( $\chi^2=0.109$  for the forces and 0.069 for the dipoles for the full set of configurations). The importance of the polarization terms to the ability to reproduce the *ab initio* forces is illustrated by showing the forces for the best pair potential obtained by force matching to the same *ab initio* forces, i.e., by just including the square-bracketed terms in Eq. (12). The representation of the forces is clearly poorer and gives an objective function value of 0.645. The forces predicted by the Fumi–Tosi effective pair potential,<sup>16,17</sup> which gives  $\chi^2=1.250$ , are also shown. Given the relatively poor prediction of the forces it is remarkable that the Fumi–Tosi potentials give many liquid and solid-state properties of the alkali chlorides as well as has been found in many previous publications (see also below).

Force matching to DFT generated forces does not allow the  $C_6$  and  $C_8$  dispersion parameters to be determined. These are fixed by requiring that an *NPT* simulation<sup>36</sup> of the fluid gives the experimental density at one temperature; the values of  $C_6$  and  $C_8$  which are found by these means are similar to those found from highly correlated electronic structure calculations on in-crystal ions.<sup>37</sup> Recently, it has been shown how the dispersion parameters for molecules can be predicted just from a knowledge of the polarizability;<sup>38</sup> we will examine this extension in the future in the hope of removing all dependence on empirical information from the procedure.

The full form of the interaction potentials and the parameters for each material are given in Appendix D.

#### IV. THE SIMULATIONS

The simulations were run on systems containing 512 ions at constant volume; as we explained above the dispersion terms in the potentials were set to ensure they give the experimental densities<sup>39</sup> (LiCl: 1.364 84 g cm<sup>-3</sup>; NaCl: 1.433 52; KCl: 1.3784) at zero pressure. The temperature was controlled with a weak Nosé–Hoover thermostat<sup>36</sup> with a relaxation time of about 5 ps, much longer than the relaxation times of the time correlation functions used to calculate the physical quantities. The simulations were run in sectors

TABLE I. Values obtained with the polarizable potentials for various subsidiary quantities are compared with experiment values (Ref. 40) (expt) and with those calculated with the Fumi–Tosi effective pair potentials (ft).  $\kappa$  is the electrical conductivity (in  $\Omega^{-1}$  cm<sup>-1</sup>);  $\eta$  is the shear viscosity (in Pa s);  $D_+$  and  $D_-$  are the diffusion coefficients of cation and anion (in cm<sup>2</sup> s<sup>-1</sup>);  $c_p$  is the constant pressure specific heat capacity (in J K<sup>-1</sup> kg<sup>-1</sup>).

| System        | $\kappa$ | $\eta \times 10^4$ | $D_+ \times 10^4$ | $D_- \times 10^4$ | $c_p$ |
|---------------|----------|--------------------|-------------------|-------------------|-------|
| LiCl (1200 K) | 6.03     | 7.78               | 1.62              | 0.936             | 1496  |
| LiCl-expt     | 7.13     | 7.37               | 2.03              | 0.951             | 1471  |
| LiCl-ft       | 7.36     | 8.26               | 1.58              | 1.10              | 1566  |
| NaCl (1300 K) | 3.71     | 7.21               | 1.28              | 1.03              | 1188  |
| NaCl-expt     | 4.10     | 6.81               | 1.32              | 1.07              | 1181  |
| NaCl-ft       | 3.91     | 6.37               | 1.15              | 1.05              | 1180  |
| KCl (1300 K)  | 2.65     | 5.75               | 1.23              | 1.16              | 913.0 |
| KCl-expt      | 2.73     | 6.26               | 1.25              | 1.14              | 982.1 |
| KCl-ft        | 3.00     | 6.22               | 1.09              | 1.11              | 923.0 |

of 500 000 steps of 0.5 fs, as we were keen to establish error bars for statistical errors on the thermal conductivity values. As we shall see, 21 such sectors were required to obtain reliable results for LiCl. One sector was run to equilibrate the system before collecting data and successive sectors were started from the final configuration of the preceding run. Simulations were run with the polarizable potentials (denoted “dippim”) and also with the Fumi–Tosi potentials which have been used to calculate thermal conductivity values for the alkali chlorides previously.<sup>9,15</sup> The various contributions to the energy flux were calculated on the fly and output for subsequent analysis.

In order to benchmark the polarizable potentials we have calculated electrical conductivity, viscosity, and diffusion coefficients, and also values for the specific heat capacity. The latter was obtained by running additional zero pressure simulations at  $\pm 50$  K from the target temperature and taking differences between the average internal energy values. The heat capacity is needed to convert the thermal conductivity to the thermal diffusivity, which is the quantity which has actually been measured for the alkali halides.<sup>5</sup> The electrical conductivity was calculated from the time integral of  $L_{zz}$ ,

$$\kappa = \frac{L_{zz}}{T}, \quad (18)$$

and also from the slope of the mean-square displacement of the charge density, the values agreeing to better than 1%. The viscosity was calculated by averaging over the integrals of the correlation functions of the five independent components of the shear stress tensor. The values for these quantities may be compared with experimental results to establish the validity of the interaction potentials, see Table I.

The comparison with the experimental data for NaCl and KCl is extremely good. For LiCl the potential predicts too small a value for the electrical conductivity (by about 15%), and examination of the diffusion coefficients suggests that this may be associated with an underestimate of the rate of diffusion of the  $\text{Li}^+$  ion. Better agreement for LiCl has been obtained previously with semiempirical polarizable potentials,<sup>18</sup> and we will investigate this further in future work. Overall, the level of agreement with experiment is very similar to that obtained with the Fumi–Tosi potentials when the latter simulations are performed at the experimental density. The properties calculated with these effective pair potentials are remarkably good, especially when one notes the level of disagreement between the *ab initio* forces and those obtained with the these potentials (Fig. 1).

## V. RESULTS FOR THE THERMAL CONDUCTIVITIES

Auto- and cross-correlation functions of the energy and charge current were calculated. As we show in Fig. 2, the shapes of these functions calculated with the different potentials are very similar. Those calculated for the Fumi–Tosi potentials are very similar to the correlation functions illustrated in previous work.<sup>20</sup>

The calculation of the thermal conductivity, obtained by combining the integrals of these functions [Eqs. (1) and (2)], seems to be bedevilled by statistical problems. Although the

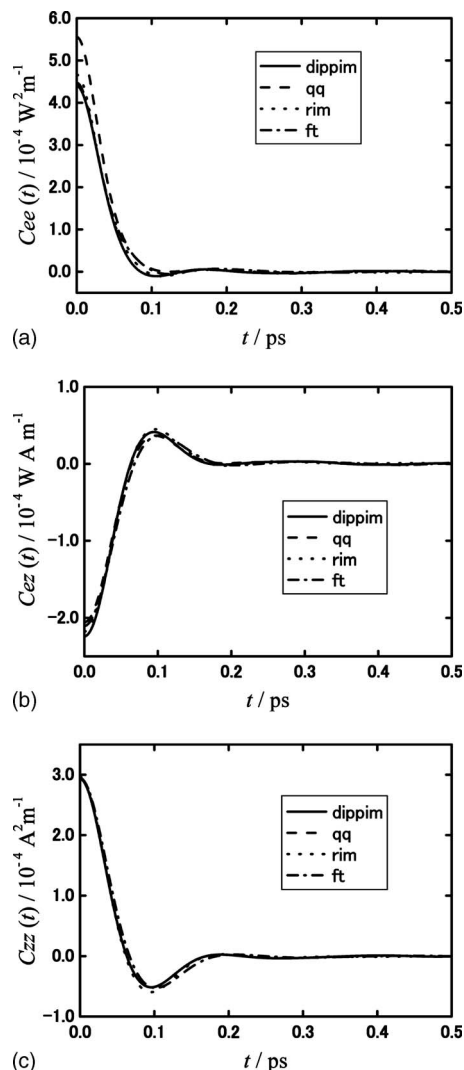


FIG. 2. The time correlation functions of the fluxes involved in the calculation of the thermal conductivity for NaCl [cf. Eq. (2)] calculated for the various potentials referred to in the text. The curves are labeled dippim: the dipole-polarizable potential; qq: omitting all dipole contributions to the heat flux in the dippim simulations; rim: omitting the polarization contributions to the interaction potentials; ft: values obtained in this work with the Fumi–Tosi potential (Refs. 16 and 17).

time correlation function of the energy and charge currents relax rapidly, obtaining an accurate value for the integrals is surprisingly difficult, and this may become serious as we must take the difference between them to obtain the thermal conductivity, as in Eq. (1). The problem is illustrated in Fig. 3 where we show the running integrals of the energy current correlation function for LiCl calculated for each of 21 sectors. Similar results were obtained for the other correlation functions and for all the potentials obtained in the study. It is clear that an estimate of the plateau value from a single sector of 500 000 steps could be subject to substantial error, although the average of the running integrals over the 21 sectors, shown by the heavy line, is well behaved. To establish a definite procedure, we define the plateau value for each sector as the average of the integrated correlation functions from 1–2 ps and averaging over the values obtained for the different sectors. We then combine the means as in Eq. (1).

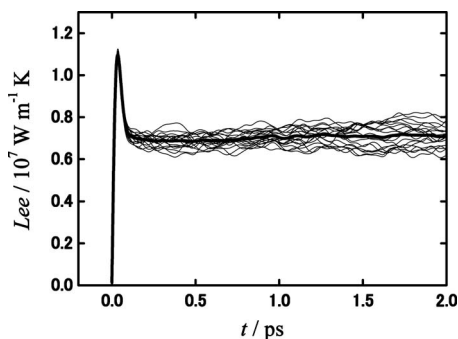


FIG. 3. The running integrals of the energy current correlation functions calculated from the data for each of 21 sectors for LiCl are shown. The heavy line indicates the average.

The values are given in Tables II–IV. The calculation of the thermal conductivity for LiCl is particularly vexatious. As the data in the table indicate, the two contributions to Eq. (1) almost cancel for this system, so that the net result is the difference of two large terms, and therefore subject to large errors. This problem is associated with the large mass difference between the ions in the LiCl case; artificially making the masses of both ions equal changes the balance of the two terms dramatically.

For the dippim simulations of KCl the agreement with experiment is perfect, for NaCl there is a 6% overestimate, and for LiCl a 17% overestimate. In all three cases, the agreement is within the combined error estimates of the experiment and the simulation but, given the fact that there are significant discrepancies for the other transport coefficients (Table I) for LiCl, we expect that the difference could be largely removed by further improvement in the potential. The experimental values for the thermal conductivity come from the forced Rayleigh experiments of Nagasaka *et al.*<sup>5</sup> This experiment actually measures the thermal diffusivity, from which the thermal conductivity was obtained by dividing by the experimental specific heat capacity and density. We have seen that, with the exception of  $c_p$  for KCl, where there is a  $\sim 10\%$  discrepancy, the simulation reproduces the experimental value for  $c_p$  very well (Table I) and the simulations were carried out at the experimental density.

Comparisons of the experimental and calculated values for the thermal conductivity show that the calculations with the polarizable potentials (dippim) improve upon those with the Fumi–Tosi (ft) potentials quite significantly. Our results

for the Fumi–Tosi potentials agree closely with published results<sup>9,15,20,41</sup> and are systematically higher than the experimental data. We also performed calculations with a RIM pair potential, which we will use to illustrate the significance of the polarization contributions to the thermal conductivity. It is obtained from the *ab initio* dippim potential by omitting the polarization component: note that this potential is *not* the “best RIM” potential described in Sec. III, it is a slightly worse potential as judged by the ability to represent the *ab initio* forces, although better than the Fumi–Tosi by this measure. Nevertheless, this potential gives quite similar results for  $\lambda$  to the Fumi–Tosi potentials. This result is included as one way of illustrating that the polarization terms have a large effect on the calculated values of  $\lambda$ .

A more direct way, than comparing results with pair and polarizable potentials, to demonstrate the importance of the polarization terms to the calculation of  $\lambda$  should be to compare the full (dippim) values with those obtained from the same simulation trajectories but with omission of the induced-dipole contributions to the heat flux. The latter are denoted “qq” in the tables. This indicates a substantial contribution from the polarization terms to the heat flux [Note, however, that this is only indicative. The fact that these values are larger than those calculated with the pair potentials (ft and rim) despite the fact that the interaction potential itself is giving a more accurate representation of the forces, indicates that it is important to be using an expression for the energy flux which is consistent with the underlying forces.]

We have seen (Table I) that the quality of agreement with experimental transport properties obtained with the polarizable and Fumi–Tosi potentials was quite similar for the electrical conductivity, viscosity, and diffusion coefficients, but that the thermal conductivity values obtained with the polarizable potentials are significantly lower and in better agreement with experiment. It seems that any pair potential which gives at least as good a representation of the *ab initio* forces as the Fumi–Tosi one (like the best RIM or the rim potential for which results were given above) will give a similarly good representation of the structure of an MX melt and of those transport properties which depend on configurational relaxation (like diffusion). Given this, it is interesting to speculate on why the results for the thermal conductivity are so much better with the polarizable potentials. It seems clear that the value of the thermal conductivity is affected by different aspects of the ionic dynamics than the

TABLE II. Calculation of the thermal conductivity for LiCl, using different interaction models, and from experiments (Ref. 5). The rows are labeled in the same way as the different curves in Fig. 2, Expt. refers to the experimental value. The column labels are explained in the text, except for “statistics” which indicates the number of simulation sectors of 500 000 steps over which averages have been performed. All quantities are given in SI units.

| LiCl<br>1200 K | $\lambda$ | $\frac{L_{ee}}{T^2}$ | $\frac{L_{ze}^2}{L_{zz}T^2}$ | $L_{zz} \times 10^{-5}$ | $L_{ze} \times 10^{-6}$ | Statistics |
|----------------|-----------|----------------------|------------------------------|-------------------------|-------------------------|------------|
| dippim         | 0.643     | 4.965                | 4.324                        | 7.187                   | -2.115                  | 21         |
| qq             | 1.321     | 4.998                | 3.676                        | 7.187                   | -1.951                  | 21         |
| rim            | 0.841     | 4.464                | 3.624                        | 6.145                   | -1.791                  | 12         |
| ft             | 0.862     | 5.623                | 4.762                        | 8.781                   | -2.454                  | 20         |
| Expt.          | 0.534     | ...                  | ...                          | ...                     | ...                     | ...        |

TABLE III. Calculation of the thermal conductivity for NaCl, using different interaction models, and from experiments (Ref. 5). The symbols are explained in the caption to Table II.

| NaCl<br>1300 K | $\lambda$ | $\frac{L_{ee}}{T^2}$ | $\frac{L_{ze}^2}{L_{zz}T^2}$ | $L_{zz} \times 10^{-5}$ | $L_{ze} \times 10^{-6}$ | Statistics |
|----------------|-----------|----------------------|------------------------------|-------------------------|-------------------------|------------|
| dippim         | 0.509     | 0.673                | 0.166                        | 4.955                   | -0.373                  | 11         |
| qq             | 0.763     | 0.893                | 0.130                        | 4.955                   | -0.330                  | 11         |
| rim            | 0.581     | 0.737                | 0.156                        | 4.537                   | -0.346                  | 10         |
| ft             | 0.558     | 0.722                | 0.166                        | 4.999                   | -0.375                  | 10         |
| Expt.          | 0.478     | ...                  | ...                          | ...                     | ...                     | ...        |

other transport coefficients, such as the viscosity or conductivity which involve structural relaxation, and therefore test the interaction model in different ways.

Recently Ohtori *et al.*<sup>41</sup> analyzed the results for the thermal conductivity of alkali halides calculated with the Fumi–Tosi potentials across a wide range of thermodynamic states and have demonstrated that they all scale very simply with the reduced mass of the ions and the number density. Properties such as the diffusion coefficient and the viscosity, which involve configurational relaxation, have a much more complex scaling behavior. A simple scaling with reduced mass and density is consistent with the hypothesis that the heat transport in these Coulomb liquids is dominated by the charge-density modes of the melt<sup>6</sup> (analogous to the optic phonons of a crystal). This provides a convenient way of rationalizing our findings about the relative sensitivity of the thermal conductivity to the presence or the absence of polarization terms in the interaction potential, compared to the other transport properties. With a pair potential the charge-density mode frequency is primarily affected by the reduced mass of the ions and the interionic separation<sup>6</sup> and depends only weakly on other properties of the interaction potential. On the other hand, when passing from a pair potential to a polarizable one, we expect the charge-density mode frequency to be reduced by (roughly) the square root of the high-frequency dielectric permittivity associated with the polarizability of the ions.<sup>42</sup> A typical value for this permittivity is 2, predicting a reduction in the predicted values for  $\lambda$  by a factor of  $\sim 1.4$  comparable to that we have found by inclusion of polarization effects.

A corollary of this and the observed insensitivity of the other transport coefficients to the exact form of the pair potential is that in the alkali halides we would expect that adding the polarization terms to the Fumi–Tosi potentials would improve the thermal conductivities without a substantial effect on structure or other transport properties.

## VI. CONCLUSIONS

We have shown how the thermal conductivity of an ionic material described by a polarizable interaction potential may be calculated by the Green–Kubo method using an appropriate expression for the energy current in a periodically replicated system. Interaction potentials of this type may be parametrized directly from *ab initio* electronic structure calculations to make the method a way of predicting the thermal conductivities for materials where an experimental determination is difficult. The results obtained for the alkali chlorides with the present dipole polarizable potentials using a fixed anion polarizability agree well with the experimental data, the largest discrepancy is only about 17% over all the transport properties of all alkali halides. The agreement for the thermal conductivity is substantially better than obtained with the well-established Fumi–Tosi effective pair potentials, and we discussed a possible physical explanation for this.

Although the agreement with experiment is probably within the combined error bounds of experiment and simulation, the systematic discrepancies, especially for LiCl, could probably be improved by further refinements of the interaction model, perhaps guided by the quality of the reproduction of the charge-density modes (or the optic phonons of the crystal).

## ACKNOWLEDGMENTS

We are very grateful to a referee for his careful reading of the original manuscript and for pointing out several errors in it. Our collaboration has been supported by a grant to PAM from the Japan Society for the Promotion of Science and to NO from the MEXT-Japan. The work was partially supported by EPSRC Grant GR/T23268/01 and by Grant-in-Aid for Scientific Research (c), 17550175 from the MEXT. M.S. acknowledges PCR-RSF and PACEN programmes for financial support.

TABLE IV. Calculation of the thermal conductivity for KCl, using different interaction models, and from experiments (Ref. 5). The symbols are explained in the caption to Table II.

| KCl<br>1300 K | $\lambda$ | $\frac{L_{ee}}{T^2}$ | $\frac{L_{ze}^2}{L_{zz}T^2}$ | $L_{zz} \times 10^{-5}$ | $L_{ze} \times 10^{-6}$ | Statistics |
|---------------|-----------|----------------------|------------------------------|-------------------------|-------------------------|------------|
| dippim        | 0.343     | 0.354                | 0.010                        | 3.352                   | -0.077                  | 11         |
| qq            | 0.499     | 0.513                | 0.014                        | 3.352                   | -0.087                  | 11         |
| rim           | 0.387     | 0.393                | 0.006                        | 3.165                   | -0.058                  | 10         |
| ft            | 0.407     | 0.413                | 0.006                        | 3.892                   | -0.064                  | 10         |
| Expt.         | 0.345     | ...                  | ...                          | ...                     | ...                     | ...        |

## APPENDIX A: DERIVATION OF THE ENERGY FLUX FOR A FLUID OF CHARGED PARTICLES

We begin with an expression for the energy density suitable for use in a periodic system:

$$\epsilon(\vec{r}) = \sum_i \frac{1}{2} m_i v_i^2 \delta(\vec{r} - \vec{r}_i) + \frac{1}{2} \rho_c(\vec{r}) \phi(\vec{r}) + \rho_{\text{self}}(\vec{r}), \quad (\text{A1})$$

where  $\vec{r}_i$  and  $\vec{v}_i$  are the positions (within the basic simulation cell) and velocities of ion  $i$  and  $\rho_c(\vec{r})$  is the local charge density at  $\vec{r}$ ,  $\sum_i z_i \delta(\vec{r} - \vec{r}_i)$ , with  $z_i$  the ionic charge.  $\phi(\vec{r})$  is the local electrical potential appropriate to a periodic system expressed<sup>12</sup> through the Ewald construction as a sum of real-space and reciprocal space terms together with a self-energy arising from the interaction between the point charge of each ion and the neutralizing Gaussian charge distribution introduced in the Ewald construction. This self-energy is removed in the expression for the energy density. The total potential energy is

$$U = \int_V d\vec{r} \left[ \frac{1}{2} \rho_c(\vec{r}) \phi(\vec{r}) + \rho_{\text{self}}(\vec{r}) \right]. \quad (\text{A2})$$

Inserting the appropriate expressions for the terms in  $\phi$  and  $\rho_{\text{self}}$ ,<sup>12</sup> we obtain

$$\begin{aligned} \epsilon(\vec{r}) &= \sum_i \frac{1}{2} m_i v_i^2 \delta(\vec{r} - \vec{r}_i) + \frac{1}{2} \sum_{i,j \neq i} z_i z_j \frac{\text{erfc}(\alpha|\vec{r} - \vec{r}_j|)}{|\vec{r} - \vec{r}_j|} \\ &\quad \times \delta(\vec{r} - \vec{r}_i) - \sum_i \frac{\alpha}{\sqrt{\pi}} z_i^2 \delta(\vec{r} - \vec{r}_i) \\ &\quad + \frac{1}{2} \sum_{i,j} z_i z_j \sum_{\vec{k} \neq 0} \frac{4\pi \exp(-k^2/4\alpha^2)}{V k^2} \\ &\quad \times \exp(i\vec{k} \cdot (\vec{r} - \vec{r}_j)) \delta(\vec{r} - \vec{r}_i), \end{aligned} \quad (\text{A3})$$

where the Ewald damping parameter and  $\alpha$  is large enough for the complementary error function  $\text{erfc}$  to die away within the length of the simulation cell. The Coulomb energy becomes

$$U = \frac{1}{2} \sum_{i,j \neq i} g_{ij}(r_{ij}) + \frac{1}{2} \sum_{i,j} \sum_{\vec{k} \neq 0} f_{ij}(k) \exp(i\vec{k} \cdot \vec{r}_{ij}) + \sum_i \epsilon_i^{\text{self}}, \quad (\text{A4})$$

this being the normal expression for the total Coulomb energy in a periodic system,<sup>12</sup> where

$$g_{ij}(r_{ij}) = z_i z_j \frac{\text{erfc}(\alpha r_{ij})}{r_{ij}}, \quad (\text{A5})$$

$$f_{ij}(k) = z_i z_j \frac{4\pi \exp(-k^2/4\alpha^2)}{V k^2}, \quad (\text{A6})$$

$$\epsilon_i^{\text{self}} = -\frac{\alpha}{\sqrt{\pi}} z_i^2. \quad (\text{A7})$$

The Fourier transformation of  $\epsilon(\vec{r})$  is

$$\epsilon(\vec{q}) = \int_V d\vec{r} \exp(i\vec{q} \cdot \vec{r}) \epsilon(\vec{r}) \quad (\text{A8})$$

$$\begin{aligned} &= \sum_i \frac{1}{2} m_i v_i^2 \exp(i\vec{q} \cdot \vec{r}_i) + \sum_i \epsilon_i^{\text{self}} \exp(i\vec{q} \cdot \vec{r}_i) \\ &\quad + \frac{1}{2} \sum_{i,j \neq i} g_{ij}(r_{ij}) \exp(i\vec{q} \cdot \vec{r}_i) \\ &\quad + \frac{1}{2} \sum_{i,j} \sum_{\vec{k} \neq 0} f_{ij}(k) \exp(i\vec{k} \cdot \vec{r}_{ij}) \exp(i\vec{q} \cdot \vec{r}_i). \end{aligned} \quad (\text{A9})$$

We require the time derivative of the Fourier component of the energy density for small wavevectors (i.e.,  $qL \ll 1$ ). We define

$$\begin{aligned} \epsilon_i^c &= \frac{1}{2} m_i v_i^2 + \epsilon_i^{\text{self}} + \frac{1}{2} \sum_j \sum_{\vec{k} \neq 0} f_{ij}(k) \exp(i\vec{k} \cdot \vec{r}_{ij}) \\ &\quad + \frac{1}{2} \sum_{j \neq i} g_{ij}(r_{ij}), \end{aligned} \quad (\text{A10})$$

and differentiate  $\epsilon(\vec{q})$  with respect to time,

$$\begin{aligned} \dot{\epsilon}(\vec{q}) &= \sum_i i\vec{q} \cdot \vec{v}_i \epsilon_i^c \exp(i\vec{q} \cdot \vec{r}_i) + \sum_i m_i \vec{v}_i \cdot \vec{v}_i \exp(i\vec{q} \cdot \vec{r}_i) \\ &\quad + \frac{1}{2} \sum_{i,j} \sum_{\vec{k} \neq 0} f_{ij}(k) \exp(i\vec{q} \cdot \vec{r}_i) i\vec{k} \cdot \vec{v}_{ij} \exp(i\vec{k} \cdot \vec{r}_{ij}) \\ &\quad + \frac{1}{2} \sum_{i,j \neq i} \exp(i\vec{q} \cdot \vec{r}_i) \vec{v}_{ij} \cdot \vec{\nabla}_{ij} g_{ij}(r_{ij}). \end{aligned} \quad (\text{A11})$$

The Coulomb contribution to the acceleration is

$$\begin{aligned} m_1 \dot{v}_{1,x} &= -\frac{\partial U}{\partial r_{1,x}} = -\frac{1}{2} \sum_j \sum_{\vec{k} \neq 0} f_{1j}(k) i\vec{k}_x \exp(i\vec{k} \cdot \vec{r}_{1j}) \\ &\quad - \exp(i\vec{k} \cdot \vec{r}_{j1}) - \sum_{j \neq 1} \nabla_{1j,x} g_{1j}(r_{1j}). \end{aligned} \quad (\text{A12})$$

When Eq. (A12) is substituted into Eq. (A11), we obtain

$$\begin{aligned} \dot{\epsilon}(\vec{q}) &= \sum_i i\vec{q} \cdot \vec{v}_i \epsilon_i \exp(i\vec{q} \cdot \vec{r}_i) + \frac{1}{2} \sum_{ij} \exp(i\vec{q} \cdot \vec{r}_i) \sum_{\vec{k} \neq 0} f_{ij}(k) \\ &\quad \times [i\vec{k} \cdot \vec{v}_i \exp(-i\vec{k} \cdot \vec{r}_{ij}) - i\vec{k} \cdot \vec{v}_j \exp(i\vec{k} \cdot \vec{r}_{ij})] \\ &\quad - \frac{1}{2} \sum_{i,j \neq i} \exp(i\vec{q} \cdot \vec{r}_i) (\vec{v}_i + \vec{v}_j) \cdot \vec{\nabla}_{ij} g_{ij}(r_{ij}). \end{aligned} \quad (\text{A13})$$

The final term in Eq. (A13) is of the same form as obtained for the contribution to the energy flux from a short-range interaction potential [note that the range of  $g_{ij}(r_{ij})$  is short with  $\alpha$  chosen appropriately] and may be transformed into the virial-like form using the usual manipulation<sup>6</sup> and the recognition that, since  $q^{-1}$  is much larger than the length of the simulation cell,  $(1 - \exp(-i\vec{q} \cdot \vec{r}_{ij})) \approx i\vec{q} \cdot \vec{r}_{ij}$ . The reciprocal space term may also be re-expressed in a similar way, as is most readily seen by writing it out explicitly for just two particles and rearranging

$$\begin{aligned}
\dot{\epsilon}(\vec{q}) &= \sum_i \exp(i\vec{q} \cdot \vec{r}_i) \\
&\times \left( i\vec{q} \cdot \vec{v}_i \epsilon_i - \frac{1}{2} \sum_{j \neq i} i\vec{q} \cdot \vec{r}_{ij} \vec{v}_i \cdot \vec{\nabla}_{ij} g_{ij}(r_{ij}) \right) \\
&+ \frac{1}{2} \sum_{ij} \exp(i\vec{q} \cdot \vec{r}_i) \sum_{\vec{k} \neq \vec{0}} f_{ij}(k) (i\vec{k} \cdot \vec{v}_i) (i\vec{q} \cdot \vec{r}_{ij}) \\
&\times \exp(-i\vec{k} \cdot \vec{r}_{ij}). \tag{A14}
\end{aligned}$$

We therefore see that  $\dot{\epsilon}(\vec{q})$  has the form appropriate to the decay of a conserved quantity,<sup>6</sup> i.e.,

$$\dot{\epsilon}(\vec{q}) = i\vec{q} \cdot (\vec{j}_e^{\text{real}}(\vec{q}) + \vec{j}_e^{\text{recip}}(\vec{q})), \tag{A15}$$

where  $i\vec{q} \cdot \vec{j}_e^{\text{recip}}$  corresponds to the final term in Eq. (A14) and  $i\vec{q} \cdot \vec{j}_e^{\text{real}}$  to the other terms.

The expression for  $i\vec{q} \cdot \vec{j}_e^{\text{recip}}$  may be transformed to a more convenient form by noting that only even terms in  $\vec{k}$ , which arise from the imaginary part of  $\exp(-i\vec{k} \cdot \vec{r}_{ij})$ , contribute to the sum over  $\vec{k}$  and therefore that the sum may be completed by including a  $\vec{k}=\vec{0}$  term, with value zero, and converted to an integral. We therefore obtain

$$\begin{aligned}
i\vec{q} \cdot \vec{j}_e^{\text{recip}} &= -\frac{1}{2} \sum_{ij} \exp(i\vec{q} \cdot \vec{r}_i) \frac{V}{8\pi^3} \\
&\times \int d\vec{k} f_{ij}(k) (i\vec{k} \cdot \vec{v}_i) (i\vec{q} \cdot \vec{\nabla}_{ij}) \exp(-i\vec{k} \cdot \vec{r}_{ij}) \\
&= \frac{1}{2} \sum_{ij} \exp(i\vec{q} \cdot \vec{r}_i) \frac{V}{8\pi^3} \\
&\times \int d\vec{k} \exp(-i\vec{k} \cdot \vec{r}_{ij}) i\vec{q} \cdot \vec{\nabla}_{ij} [f_{ij}(k) (i\vec{k} \cdot \vec{v}_i)], \tag{A16}
\end{aligned}$$

where the second step is obtained by an integration over parts. Finally, substituting the expression for  $f_{ij}(k)$ , carrying out the differentiation explicitly, and converting the integral back to a sum, we obtain

$$\begin{aligned}
i\vec{q} \cdot \vec{j}_e^{\text{recip}} &= \frac{1}{2} \sum_{\vec{k} \neq \vec{0}} \sum_{ij} \exp(i\vec{q} \cdot \vec{r}_i) z_i z_j \frac{4\pi \exp(-k^2/4\alpha^2)}{V k^2} \\
&\times \left[ i\vec{q} \cdot \vec{v}_i - (\vec{k} \cdot \vec{v}_i) (i\vec{q} \cdot \vec{k}) \left( \frac{k^2 + 4\alpha^2}{2\alpha^2 k^2} \right) \right] \\
&\times \exp(-i\vec{k} \cdot \vec{r}_{ij}), \tag{A17}
\end{aligned}$$

where the  $\vec{k}=\vec{0}$  term is omitted because it makes no contribution for a charge-neutral system.

## APPENDIX B: RELATIONSHIP BETWEEN EXPRESSIONS FOR THE ENERGY CURRENT

The purpose of this appendix is to explore the relationship between the expression for the energy flux derived by Bernu and Viellefosse<sup>14</sup> and that proposed by Galamba *et al.*<sup>15</sup> We begin with an expression for the Coulombic contributions to the  $x$ -component of the energy flux as given in Eq. (A3) of Bernu and Viellefosse with  $\beta=1$ ,

$$\begin{aligned}
j_{e,x} &= \sum_{i,j \neq i} \left[ \frac{1}{2} \left( v_{ix} + r_{ijx} \frac{\vec{v}_i \cdot \vec{r}_{ij}}{r_{ij}^2} \right) \left( \frac{\text{erfc}(\alpha r_{ij})}{r_{ij}} \right. \right. \\
&\quad \left. \left. + \frac{2\alpha}{\sqrt{\pi}} \exp(-\alpha^2 r_{ij}^2) \right) - \frac{2\pi}{V \alpha^2} v_{ix} \right] \\
&+ \sum_{ij} \frac{4\pi}{V} \sum_{\vec{k} \neq \vec{0}} \frac{\exp(-k^2/4\alpha^2 - i\vec{k} \cdot \vec{r}_{ij})}{k^2} \left( \left( 1 - \frac{k^2}{4\alpha^2} \right) v_{ix} \right. \\
&\quad \left. - \left( 1 + \frac{k^2}{4\alpha^2} \right) \frac{k_x \vec{v}_i \cdot \vec{k}}{k^2} \right), \tag{B1}
\end{aligned}$$

where we have included explicit charges on the two species and transformed the notation into that of the current paper, i.e.,

$$\vec{k} = \frac{2\pi}{L} \vec{r}, \quad r_{ij} = L \times r_{ij}, \quad \alpha = \frac{\alpha}{L}, \tag{B2}$$

where the terms on the right-hand side are those of Bernu and Viellefosse, and those on the left are ours. In addition to these trivial changes, we have made one substantial change which is to include the sum over *all*  $i$  and  $j$  in the reciprocal space summation, whereas the original paper indicates  $i \neq j$ . We believe that this is a misprint in the original article, as it becomes impossible to use the Ewald construction with  $i \neq j$ , and it has always been interpreted as such in previous calculations of the energy flux.<sup>20</sup>

We now note that

$$\begin{aligned}
\frac{\alpha}{\sqrt{\pi}} \exp(-\alpha^2 r_{ij}^2) &= \frac{4\pi}{V} \left( \frac{1}{4\alpha^2} + \sum_{\vec{k} \neq \vec{0}} \frac{\exp(-k^2/4\alpha^2 - i\vec{k} \cdot \vec{r}_{ij})}{4\alpha^2} \right), \tag{B3}
\end{aligned}$$

which can be shown by converting the term in brackets into the integral over all  $\vec{k}$ . By making use of this identity we obtain

$$\begin{aligned}
j_{e,x} = & \frac{1}{2} \sum_{i,j \neq i} \frac{\operatorname{erfc}(\alpha r_{ij})}{r_{ij}} v_{ix} + \frac{1}{2} \sum_{i,j \neq i} r_{ijx} \frac{\vec{v}_i \cdot \vec{r}_{ij}}{r_{ij}^2} \\
& \times \left( \frac{\operatorname{erfc}(\alpha r_{ij})}{r_{ij}} + \frac{2\alpha}{\sqrt{\pi}} \exp(-\alpha^2 r_{ij}^2) \right) \\
& + \frac{4\pi}{V} \sum_{i,j} \sum_{\vec{k} \neq \vec{0}} \frac{\exp(-k^2/4\alpha^2 - i\vec{k} \cdot \vec{r}_{ij})}{k^2} \\
& \times \left( v_{ix} - \left( 1 + \frac{k^2}{4\alpha^2} \right) \frac{k_x \vec{v}_i \cdot \vec{k}}{k^2} \right), \\
& - \sum_i \left( \frac{\alpha}{\sqrt{\pi}} - \frac{\pi}{V\alpha^2} \right) z_i^2 v_{ix} - \sum_{i,j \neq i} \frac{\pi v_{ix}}{V\alpha^2}, \quad (\text{B4})
\end{aligned}$$

where the term in  $z_i^2$  comes from the noncanceling  $i=j$  term. The Coulomb contribution to the energy per particle,  $\epsilon_i^c$ , is given by Eq. (9) and the real-space Coulomb force between  $i$  and  $j$ ,  $\vec{f}_{ij}^{\text{real}}$ , by Eq. (10). Introducing these expressions we obtain

$$\begin{aligned}
j_{e,x} = & \sum_i \epsilon_i^c v_{ix} + \frac{1}{2} \sum_{i,j \neq i} r_{ijx} \vec{v}_i \cdot \vec{f}_{ij}^{\text{real}} \\
& + \frac{1}{2} \frac{4\pi}{V} \sum_{i,j} \sum_{\vec{k} \neq \vec{0}} \frac{\exp(-k^2/4\alpha^2 - i\vec{k} \cdot \vec{r}_{ij})}{k^2} \\
& \times \left( v_{ix} - \left( 2 + \frac{k^2}{2\alpha^2} \right) \frac{k_x \vec{v}_i \cdot \vec{k}}{k^2} \right) \\
& + 2 \sum_i \frac{\pi}{V\alpha^2} z_i^2 v_{ix} - \sum_i z_i \frac{\pi v_{ix}}{V\alpha^2} \sum_j z_j. \quad (\text{B5})
\end{aligned}$$

We now recognize the convective and real-space Ewald virial-like contributions to the energy flux as the first two terms on the right-hand side of this expression [cf. Eq. (8)]. The third, reciprocal space term is exactly equal to that proposed by Galamba *et al.* The final term vanishes for an electrically neutral system because it involves a sum over all charges. We therefore see that the Bernu-Viellesfosse BV equation for the energy flux (with the double-sum over all particles taken as a correction) is identical to the GNE expression except for the appearance of an additional term which involves the net velocity of each species

$$\text{BV} = \text{GNE} + 2 \sum_i \frac{\pi}{V\alpha^2} z_i^2 v_{ix}. \quad (\text{B6})$$

For a 1-1 electrolyte, where  $z_i^2$  is the same for both species, the additional term is proportional to the net velocity of the simulation cell and will vanish if the ions have equal masses because of the zero net cell momentum. In other cases, one would expect a small term reflecting the net velocity of one species.

### APPENDIX C: THE ENERGY FLUX FOR CHARGED, POLARIZABLE PARTICLES

For a periodic system composed of charges and induced dipoles the expression for the energy density becomes

$$\begin{aligned}
\epsilon(\vec{r}) = & \sum_i \frac{1}{2} m_i v_i^2 \delta(\vec{r} - \vec{r}_i) + \frac{1}{2} \rho_c(\vec{r}) \phi(\vec{r}) \\
& - \frac{1}{2} \vec{M}(\vec{r}) \cdot \vec{E}(\vec{r}) + \rho_{\text{self}}(\vec{r}), \quad (\text{C1})
\end{aligned}$$

where, in addition to the terms introduced in Appendix A,  $\vec{M}(\vec{r})$  is the dipole density ( $\sum_i \vec{\mu}_i \delta(\vec{r} - \vec{r}_i)$ ) and  $\vec{E}(\vec{r})$  is the electric field appropriate to a periodic system of charges and dipoles expressed through the Ewald construction.<sup>27</sup> Note too that the electrical potential  $\phi$  now includes a contribution from dipoles as well as charges. The self-energy density

$$\rho_{\text{self}}(\vec{r}) = \sum_i e_i^{\text{self}} \delta(\vec{r} - \vec{r}_i) \quad (\text{C2})$$

involves terms arising from the interaction with the neutralising background which are overcounted in the Ewald construction (as in Appendix A, but now including a dipole term) but also the actual polarization energy of the ions, which is represented in the normal Drude construction as  $\frac{1}{2} k \mu^2$ , where  $k$  is the Drude force constant, given by the inverse of the ionic polarizability. The self-energy associated with ion  $i$  is therefore given by

$$\epsilon_i^{\text{self}} = -\frac{\alpha}{\sqrt{\pi}} z_i^2 - \frac{2\alpha^3}{3\sqrt{\pi}} \mu_i^2 + \frac{1}{2} k_i \mu_i^2. \quad (\text{C3})$$

We proceed, as in Appendix A, to introduce appropriate expressions for  $\phi$  and  $\vec{E}$ ,<sup>27</sup> and obtain expressions for the total Coulomb energy and the Fourier components of the energy density which may be written

$$U = \frac{1}{2} \sum_{i,j \neq i} G_{ij}(\vec{r}_{ij}) + \frac{1}{2} \sum_{i,j} \sum_{\vec{k} \neq \vec{0}} F_{ij}(\vec{k}) \exp(i\vec{k} \cdot \vec{r}_{ij}) + \sum_i \epsilon_i^{\text{self}} \quad (\text{C4})$$

and

$$\begin{aligned}
\epsilon(\vec{q}) = & \sum_i \frac{1}{2} m_i v_i^2 \exp(i\vec{q} \cdot \vec{r}_i) + \sum_i \epsilon_i^{\text{self}} \exp(i\vec{q} \cdot \vec{r}_i) \\
& + \frac{1}{2} \sum_{i,j \neq i} G_{ij}(\vec{r}_{ij}) \exp(i\vec{q} \cdot \vec{r}_i) \\
& + \frac{1}{2} \sum_{i,j} \sum_{\vec{k} \neq \vec{0}} F_{ij}(\vec{k}) \exp(i\vec{k} \cdot \vec{r}_{ij}) \exp(i\vec{q} \cdot \vec{r}_i). \quad (\text{C5})
\end{aligned}$$

These expressions have been written by analogy to those in Appendix A, to indicate that they may be transformed in the same way into useful forms for evaluation. Now we have

$$G_{ij}(\vec{r}_{ij}) = z_i z_j \hat{T}_{ij} - z_i \hat{T}_{ij}^\alpha \mu_{j,\alpha} + z_j \hat{T}_{ij}^\alpha \mu_{i,\alpha} + \mu_{i,\alpha} \hat{T}_{ij}^{\alpha\beta} \mu_{j,\beta}, \quad (\text{C6})$$

$$\begin{aligned}
F_{ij}(\vec{k}) = & \frac{4\pi \exp(-k^2/4\alpha^2)}{V k^2} [z_i z_j + z_i (i\vec{k} \cdot \vec{\mu}_j) - z_j (i\vec{k} \cdot \vec{\mu}_i) \\
& - (i\vec{k} \cdot \vec{\mu}_j)(i\vec{k} \cdot \vec{\mu}_i)], \quad (\text{C7})
\end{aligned}$$

which include the charge-dipole and dipole-dipole contributions to the energy alongside the charge-charge terms.  $\hat{T}_{ij}^\alpha$  etc., are the Ewald-modified real-space interaction tensors,<sup>27</sup>

$$\hat{T}_{ij} = \frac{\text{erfc}(\alpha r_{ij})}{r_{ij}}, \quad (\text{C8})$$

$$\hat{T}_{ij}^\alpha = -r_{ij,\alpha} \left[ \frac{\text{erfc}(\alpha r_{ij})}{r_{ij}^3} + \frac{2\alpha \exp(-\alpha r_{ij}^2)}{\sqrt{\pi} r_{ij}^2} \right]. \quad (\text{C9})$$

$$\begin{aligned} \hat{T}_{ij}^{\alpha\beta} = & -\delta_{\alpha,\beta} \left[ \frac{\text{erfc}(\alpha r_{ij})}{r_{ij}^3} + \frac{2\alpha \exp(-\alpha r_{ij}^2)}{\sqrt{\pi} r_{ij}^2} \right] \\ & + r_{ij,\alpha} r_{ij,\beta} \left[ 3 \frac{\text{erfc}(\alpha r_{ij})}{r_{ij}^5} + \frac{2\alpha \exp(-\alpha r_{ij}^2)}{\sqrt{\pi} r_{ij}^2} \right] \\ & \times (2\alpha^2 + 3r_{ij}^{-2}) \Big]. \quad (\text{C10}) \end{aligned}$$

As remarked above, Eqs. (C4) and (C5) have exactly the same form as the corresponding expressions in Appendix A, i.e., Eqs. (A4) and (A9). Since the time derivatives of the dipole moments are to be neglected, following the explanation given in the main text, the expression for the time derivative of the Fourier components of the energy density becomes

$$\begin{aligned} \dot{\epsilon}(\vec{q}) = & \sum_i \exp(i\vec{q} \cdot \vec{r}_i) \\ & \times \left( i\vec{q} \cdot \vec{v}_i \epsilon_i - \frac{1}{2} \sum_{j \neq i} i\vec{q} \cdot \vec{r}_{ij} \vec{v}_i \cdot \vec{\nabla}_{ij} G_{ij}(\vec{r}_{ij}) \right) \\ & + \frac{1}{2} \sum_{ij} \exp(i\vec{q} \cdot \vec{r}_i) \sum_{\vec{k} \neq 0} F_{ij}(\vec{k}) (i\vec{k} \cdot \vec{v}_i) (i\vec{q} \cdot \vec{r}_{ij}) \\ & \times \exp(-i\vec{k} \cdot \vec{r}_{ij}), \quad (\text{C11}) \end{aligned}$$

which shows that this energy density is conserved (i.e.,  $\propto i\vec{q} \cdot \vec{j}_e$ ). Here  $-\nabla_{ij} G_{ij}(\vec{r}_{ij})$  is the real-space force on ion  $i$  due to  $j$ , so that the second term acquires the virial-like form, with the force including all real-space charge and dipole interactions, and

$$\begin{aligned} \epsilon_i = & \frac{1}{2} m_i v_i^2 + \epsilon_i^{\text{self}} + \frac{1}{2} \sum_{j \neq i} G_{ij}(\vec{r}_{ij}) \\ & + \frac{1}{2} \sum_j \sum_{\vec{k} \neq 0} F_{ij}(\vec{k}) \exp(i\vec{k} \cdot \vec{r}_{ij}). \quad (\text{C12}) \end{aligned}$$

As before, the sum over  $\vec{k}$  in the last term of Eq. (C11) may be converted to an integral and evaluated by parts,

$$\begin{aligned} i\vec{q} \cdot \vec{j}_e^{\text{recip}} = & -\frac{1}{2} \sum_{ij} \exp(i\vec{q} \cdot \vec{r}_i) \frac{V}{8\pi^3} \\ & \times \int d\vec{k} F_{ij}(\vec{k}) (i\vec{k} \cdot \vec{v}_i) (i\vec{q} \cdot \vec{r}_{ij}) \exp(-i\vec{k} \cdot \vec{r}_{ij}) \\ = & \frac{1}{2} \sum_{ij} \exp(i\vec{q} \cdot \vec{r}_i) \frac{V}{8\pi^3} \\ & \times \int d\vec{k} \exp(-i\vec{k} \cdot \vec{r}_{ij}) i\vec{q} \cdot \vec{\nabla}_{\vec{k}} [F_{ij}(\vec{k}) (i\vec{k} \cdot \vec{v}_i)]. \quad (\text{C13}) \end{aligned}$$

Finally, substituting the expression for  $F_{ij}(\vec{k})$ , carrying out the differentiation explicitly, and converting the integral back to a sum, we obtain

$$\begin{aligned} i\vec{q} \cdot \vec{j}_e^{\text{recip}} = & \frac{1}{2} \sum_{\vec{k} \neq 0} \sum_{ij} \exp(i\vec{q} \cdot \vec{r}_i) \frac{4\pi \exp(-k^2/4\alpha^2)}{V k^2} \\ & \times \exp(-i\vec{k} \cdot \vec{r}_{ij}) \left( \left[ i\vec{q} \cdot \vec{v}_i - (\vec{k} \cdot \vec{v}_i) (i\vec{q} \cdot \vec{k}) \left( \frac{k^2 + 4\alpha^2}{2\alpha^2 k^2} \right) \right] \right. \\ & \times [z_i z_j + z_i (i\vec{k} \cdot \vec{\mu}_j) - z_j (i\vec{k} \cdot \vec{\mu}_i) - (i\vec{k} \cdot \vec{\mu}_j) (i\vec{k} \cdot \vec{\mu}_i)] \\ & + (i\vec{k} \cdot \vec{v}_i) [z_i (i\vec{q} \cdot \vec{\mu}_j) - z_j (i\vec{q} \cdot \vec{\mu}_i) - (i\vec{q} \cdot \vec{\mu}_j) (i\vec{k} \cdot \vec{\mu}_i) \\ & \left. - (i\vec{k} \cdot \vec{\mu}_j) (i\vec{q} \cdot \vec{\mu}_i) \right]. \quad (\text{C14}) \end{aligned}$$

## APPENDIX D: THE INTERACTION POTENTIAL

The interaction potential actually used in the liquid state simulations is a ‘‘polarizable ion model’’ and consists of a pair potential of Born–Mayer form together with an account of ionic polarization.<sup>10,24</sup> The expressions for the pair potentials are given in Eqs. (16) and (17). Values for all parameters necessary to simulate the alkali chlorides are given in Table I. All the parameters are given in au; the atomic unit of length is the Bohr radius (0.529 18 Å) and of energy the Hartree,  $4.3597 \times 10^{-18}$  J. The cation-cation potentials are very short ranged and have very little influence on the liquid structural and dynamical properties (i.e., the cations are kept apart by the Coulomb repulsion and the relatively large size of the anions). For this reason we tend to assign these potentials fixed values in order to avoid them playing a role in the fitting process.

TABLE V. Potential parameters.

| Ion pair                         | $B_{ij}$ | $\alpha_{ij}$ | $C_{ij}^6$ | $C_{ij}^8$ | $b_{ij}^6$ | $b_{ij}^8$ | $b_{+-} = b_{-+}$ | $c_+$ | $c_+$ |
|----------------------------------|----------|---------------|------------|------------|------------|------------|-------------------|-------|-------|
| Cl <sup>-</sup> –Cl <sup>-</sup> | 179.7    | 2.751         | 140        | 280        | 1.7        | 1.7        | ...               | ...   | ...   |
| Cl <sup>-</sup> –Li <sup>+</sup> | 58.85    | 1.95          | 0.0        | 0.0        | ...        | ...        | 1.861             | 2.079 | ...   |
| Cl <sup>-</sup> –Na <sup>+</sup> | 67.50    | 1.726         | 37.4       | 167.3      | 1.7        | 1.7        | 1.76              | 3.0   | 0.697 |
| Cl <sup>-</sup> –K <sup>+</sup>  | 208.6    | 1.83          | 26.4       | 118.3      | 1.7        | 1.7        | 1.632             | 3.0   | 0.917 |
| Li <sup>+</sup> –Li <sup>+</sup> | 1.0      | 5.0           | 0.0        | 0.0        | ...        | ...        | ...               | ...   | ...   |
| Na <sup>+</sup> –Na <sup>+</sup> | 1.0      | 5.0           | 10.0       | 100.0      | 1.7        | 1.7        | ...               | ...   | ...   |
| K <sup>+</sup> –K <sup>+</sup>   | 1.0      | 5.0           | 5.0        | 50.0       | 1.7        | 1.7        | ...               | ...   | ...   |

We used a chloride ion polarizability of 20 Bohrs<sup>3</sup>, and 0.89 and 4.71 Bohrs<sup>3</sup> for Na<sup>+</sup> and K<sup>+</sup>, respectively.<sup>35</sup> The charge-dipole interaction tensor is modified by applying a damping function [cf. Eq. (13)] to account for short-range contributions to the induced dipoles<sup>10,24</sup> and the values of  $c_{ij}$  and  $b_{ij}$  obtained from the fits to the *ab initio* dipoles are given in Table V. The damping function is only applied to the interactions between unlike ions (i.e., the relevant  $c_{ij}$  term is zero); including a like-like damping term is a potential refinement to the potential model, but it does introduce further parameters.

<sup>1</sup>A. M. Hofmeister, *Proc. Natl. Acad. Sci. U.S.A.* **104**, 9192 (2007).

<sup>2</sup>G. W. Goward, *Surf. Coat. Technol.* **108**, 73 (1998).

<sup>3</sup>C. Forsberg, *Prog. Nucl. Energy* **47**, 32 (2005).

<sup>4</sup>C. Le Brun, *J. Nucl. Mater.* **360**, 1 (2007).

<sup>5</sup>Y. Nagasaka, N. Nakazawa, and A. Nagashima, *Int. J. Thermophys.* **13**, 555 (1992).

<sup>6</sup>J.-P. Hansen and I. R. McDonald, *Theory of Simple Liquids* 2nd ed. (Academic, New York, 1986).

<sup>7</sup>P. Sindzingre and M. J. Gillan, *J. Phys.: Condens. Matter* **2**, 7033 (1990).

<sup>8</sup>S. S. Sarman, D. J. Evans, and P. T. Cummings, *Phys. Rep.* **305**, 1 (1998).

<sup>9</sup>N. Galamba, C. A. Nieto de Castro, and J. F. Ely, *J. Chem. Phys.* **126**, 204511 (2007).

<sup>10</sup>P. A. Madden, R. Heaton, A. Aguado, and S. Jahn, *J. Mol. Struct.: THEOCHEM* **771**, 9 (2006).

<sup>11</sup>S. Jahn and P. A. Madden, *Phys. Earth Planet. Inter.* **162**, 129 (2007).

<sup>12</sup>D. Frenkel and B. Smit, *Understanding Molecular Dynamics*, 2nd ed. (Academic, New York, 2002).

<sup>13</sup>M. P. Allen and D. J. Tildesley, *Computer Simulation of Liquids*, (Oxford Science, New York, 1989).

<sup>14</sup>B. Bernu and P. Vieillefosse, *Phys. Rev. A* **18**, 2345 (1978).

<sup>15</sup>N. Galamba, C. A. Nieto de Castro, and J. F. Ely, *J. Chem. Phys.* **120**, 8676 (2004).

<sup>16</sup>F. G. Fumi and M. P. Tosi, *J. Phys. Chem. Solids* **25**, 31 (1964).

<sup>17</sup>M. P. Tosi and F. G. Fumi, *J. Phys. Chem. Solids* **25**, 45 (1964).

<sup>18</sup>B. Morgan and P. A. Madden, *J. Chem. Phys.* **120**, 1402 (2004).

<sup>19</sup>A. Aguado, M. Wilson, and P. A. Madden, *J. Chem. Phys.* **115**, 8603 (2001).

<sup>20</sup>K. Takase and N. Ohtori, *Electrochemistry (Tokyo, Jpn.)* **67**, 581 (1999).

<sup>21</sup>S. W. de Leeuw, J. W. Perram, and E. R. Smith, *Proc. R. Soc. London, Ser. A* **373**, 27 (1980).

<sup>22</sup>F. Bresme, B. Hafskjöld, and I. Wold, *J. Phys. Chem.* **100**, 1879 (1996).

<sup>23</sup>S. Nosé and M. L. Klein, *Mol. Phys.* **50**, 1055 (1983).

<sup>24</sup>M. Wilson, P. A. Madden, and B. J. Costa Cabral, *J. Phys. Chem.* **100**, 1227 (1995).

<sup>25</sup>A. J. Stone, *Theory of Intermolecular Forces* (Oxford University Press, Oxford, 1996).

<sup>26</sup>K. T. Tang and J. P. Toennies, *J. Chem. Phys.* **80**, 3726 (1984).

<sup>27</sup>A. Aguado and P. A. Madden, *J. Chem. Phys.* **119**, 7471 (2003).

<sup>28</sup>F. Hutchinson, A. J. Rowley, M. K. Walters, M. Wilson, P. A. Madden, J. C. Wasse, and P. S. Salmon, *J. Chem. Phys.* **111**, 2028 (1999).

<sup>29</sup>M. Salanne, C. Simon, P. Turq, and P. A. Madden, *J. Phys. Chem. B* **112**, 1177 (2008).

<sup>30</sup>O. J. Lanning, S. Shellswell, and P. A. Madden, *Mol. Phys.* **102**, 839 (2004).

<sup>31</sup>R. J. Heaton, R. Brookes, P. A. Madden, M. Salanne, C. Simon, and P. Turq, *J. Phys. Chem. B* **110**, 11454 (2006).

<sup>32</sup>The CPMD consortium, CPMD Version 3.x, <http://www.cpmc.org>. MPI Fur Festkorperforschung and the IBM Zurich Research Laboratory.

<sup>33</sup>R. J. Heaton, P. A. Madden, S. J. Clark, and S. Jahn, *J. Chem. Phys.* **125**, 144104 (2006).

<sup>34</sup>M. Salanne, R. Vuilleumier, P. A. Madden, C. Simon, P. Turq, and B. Guillot, *J. Phys.: Condens. Matter* **20**, 492407 (2008).

<sup>35</sup>P. W. Fowler and P. A. Madden, *Phys. Rev. B* **29**, 1035 (1984).

<sup>36</sup>G. J. Martyna, D. Tobias, and M. L. Klein, *J. Chem. Phys.* **101**, 4177 (1994).

<sup>37</sup>P. W. Fowler, P. J. Knowles, and N. C. Pyper, *Mol. Phys.* **56**, 83 (1985).

<sup>38</sup>A. D. Becke and E. R. Johnson, *J. Chem. Phys.* **127**, 154108 (2007).

<sup>39</sup>E. R. Van Artsdalen and I. S. Yaffe, *J. Phys. Chem.* **59**, 118 (1955).

<sup>40</sup>G. Janz, *Molten Salts Handbook* (Academic, New York, 1967).

<sup>41</sup>N. Ohtori, T. Ono, and K. Takase, *J. Chem. Phys.* **130**, 044505 (2009).

<sup>42</sup>K. F. O'Sullivan and P. A. Madden, *J. Phys.: Condens. Matter* **3**, 8751 (1991).